Signal Enhancement with Stacked Magnets for High-Resolution Radio Frequency Glow Discharge Mass Spectrometry

Juan Wei,[†] Jiangli Dong,[†] Shangjun Zhuo,[†] Rong Qian,[*,†] Yuanxing Fang,[‡] Qiao Chen,[*,‡] Ekbal Patel[§]

[†]National Center for Inorganic Mass Spectrometry in Shanghai, Shanghai Institute of Ceramics, Chinese Academy of Sciences, 200050 Shanghai, P. R. China

[‡]Department of Chemistry, School of Life Sciences, University of Sussex, BN1 9QJ Brighton, UK

[§]Mass Spectrometry Instruments Ltd., UK

Key words: rf-GD-MS, self-adhesive, magnet, signal, enhancement

ABSTRACT: A method for signal enhancement utilizing stacked magnets was introduced into high-resolution radio frequency glow discharge-mass spectrometry (rf-GD-MS) for significantly improved analysis of inorganic materials. Compared to the block magnet, the stacked magnets method was able to achieve 50−59% signal enhancement for typical elements in Y_2O_3, BSO, and BTN samples. The results indicated that signal was enhanced as the increase of discharge pressure from 1.3 to 8.0 mPa, the increase of rf-power from 10 to 50 W with a frequency of 13.56 MHz, the decrease of sample thickness, and the increase of number of stacked magnets. The possible mechanism for the signal enhancement was further probed using the software "Mechanical APDL (ANSYS) 14.0". It was found that the distinct oscillated magnetic field distribution from the stacked magnets was responsible for signal enhancement, which could extend the movement trajectories of electrons and increase the collisions between the electrons and neutral particles to increase the ionization efficiency. Two NIST samples were used for the validation of the method, and the results suggested that relative errors were within 13% and detection limit for six transverse stacked magnets could reach as low as 0.0082 μg g^{-1}. Additionally, the stability of the method was also studied. RSD within 15% of the elements in three nonconducting samples could be obtained during the sputtering process. Together, the results showed that the signal enhancement method with stacked magnets could offer great promises in providing a sensitive, stable, and facile solution for analyzing the nonconducting materials.

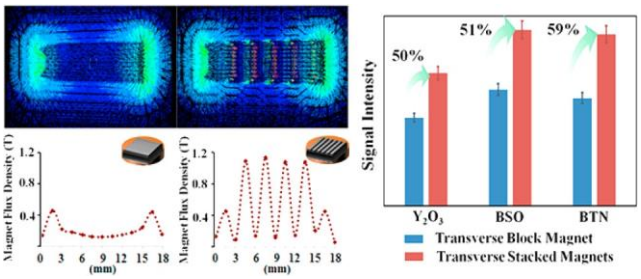

INTRODUCTION

Glow discharge mass spectrometry (GD-MS) is one of the most effective methods for direct determination of trace elements of solid materials due to high mass resolution, high sensitivity, low detection limits (down to ng g-1) and the ability to measure almost all elements with isotops. While GD-MS coupling with rf discharge, samples can be directly sputtered and ionized at lower gas pressure than in a dc discharge process.[1] Particularly, the rf-GD-MS has offered efficient depth profile analysis of different materials, such as glass, ceramics and new composite materials, thus widening its applications.[2-13]

Generally, the principles of rf glow discharge is similar to direct current glow discharge in many respects. However, as an AC potential is applied in an rf-GD process, electrical insulating samples can be effectively sputtered. In such a process, electrons and cations in the plasma are oscillated between the sample surface and the counter electrode.[14] In an rf-GD process, such negative self-bias formed on the sample surface could increase sputtering rate and ionization efficiency.[10, 16] For a mass spectrometry, the sputtering rate and ionization efficiency play important roles in achieving the optimum analytical performance,[16] which could also be influenced by other factors such as gas pressure, rf-power, sample thickness, lattice binding energy of sample and so on.[17, 18]

With radio frequency (rf) discharges, nonconducting materials can be analyzed directly. However, the generator power is usually coupled capacitive to the plasma, so that the plasma power decreases with increasing thickness, thus sputtering rates, sensitivities and signal intensity decrease at the same time.[19] In recent years, some efforts have been made to improve the ionization efficiency and detection sensitivity in GD-MS by utilization of power pulse[20] or adding external

magnetic field.[16] The benefits of the external magnetic field classified as magnetron, have been successfully exploited in a variety of spectroscopies.[16−18,21−23] For instance, Vega et al. introduced a permanent block magnet into the rf-GD chamber coupled with an optical emission spectroscopy.[17] Similarly, Saprykin et al. used a ring-shaped magnet behind the sample to improve the sensitivity of the rf-GD-MS.[21]

The added external magnetic field could modify the motion of the electrons and cations into spiral trajectory under the Lorentz forces, leading to an increased ion bombardment probability and resulting in higher sputtering rates and signal intensities.[16,24,25] Such enhancement can be significantly affected by the magnetic field strength and its spatial distribution.

In present work, an effective stacked magnetic system was designed, constructed, and applied to rf-GD-MS. In comparison with a block magnet of the same magnetizing orientation, the significant enhancement in the detection sensitivity with stacked magnets was quantitatively identified on standard insulating samples. Meanwhile, the accuracy and stability of this method was validated by NIST samples, typical ceramic, and crystal samples. The distributions of magnetic field strength from the block magnet and the stacked magnets were analyzed by Ansys magnetic field simulation. We found that the existing boundaries within stacked magnets result in an alternating distribution of the magnetic field with peaks and troughs, which is responsible for the enhancement of signal intensity in the rf-GD-MS.

EXPERIMENTAL

2.1 Construction of Magnetic System

For magnetic system, the copper shell (28 mm in diameter and 6 mm in height) was manufactured to hold magnets on the back while the sample was mounted on the front. High-power NdFeB magnets were used as the source of the magnetic field. Considering the different magnetic field might perform different influences on the movement of electrons, two orientations including transverse magnet and axial magnets were chosen for investigation and comparison. Then, the

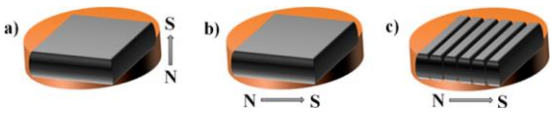

axial block magnet (20 mm × 18 mm × 5 mm), the transverse block magnet (20 mm × 18 mm × 5 mm) and several stacked magnets (20 mm × 3 mm × 5 mm for each piece)

Figure 1. Diagram of magnetic system filled with (a) the axial block magnet, (b) the transverse block magnet, and (c) the six transverse stacked magnets.

with transverse orientation were filled into the magnetic system, respectively. The coercivity of 876 kA/m was specified by the manufacturer. The mounting geometries of block and stacked magnets inside the copper shell were shown in Figure 1. As such, the magnetic field of the transverse stacked magnets and the transverse block magnet were parallel to the sample surface and perpendicular to the electric field, while that of the axial block magnet was perpendicular to the sample surface and parallel to the electric field.

2.2 Materials and Sample Preparation.

To demonstrate the enhanced performance of rf-GD-MS, three nonconducting samples were used in the present work.

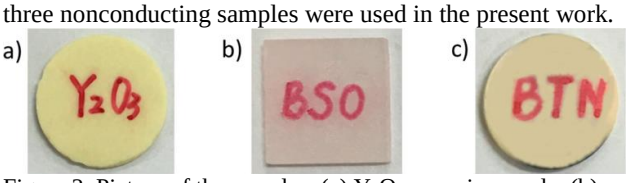

Figure 2. Picture of the samples: (a) Y_2O_3 ceramic sample, (b) BSO crystal sample, and (c) BTN ceramic sample.

Y_2O_3 sample doped with Al, Zr, Eu, Zn (Figure 2a), BSO (Bi12SiO20) sample doped with Al, Fe, Cu (Figure 2b) and BTN (Ba5.52La0.32Ti2Nb8O30) sample doped with Bi (Figure 2c) were provided by Shanghai Institute of Ceramics, Chinese Academy of Sciences. They were all manufactured into flat sample with various thicknesses (1 mm, 1.5 mm, 2 mm, and 2.5 mm). Two NIST standard reference materials 1831 and 620 (Department of Commerce, National Institution of Standards and Technology, Gaithersburg, MD) were also used to verify the method. Their certified values of constituents were listed in Table 1. During the preparation process, all the samples were cleaned with dilute nitric acid solution, deionized water, and finally cleaned with anhydrous ethanol. The prepared samples were kept in anhydrous ethanol before measurements.

2.3 rf-GD-MS Experiments.

The rf-GD-MS used in this work was the AutoConcept GD90 (Mass Spectrometry Instruments Ltd., U.K.). The ion-generating device consists of a rf power source, a sample holder inserted in a discharge chamber filled with low pressure argon (Scheme 1). The sample holder was modified including a spring loaded cylindrical magnetic device, which has a flat seat to accommodate a flat sample. The rf power was directly applied onto the copper shell through an electrical probe. High-purity argon gas (>99.9999%) was injected into the source chamber with controlled flow rates. The high vacuum was maintained by turbo pumps.

Scheme 1. Diagram of discharge chamber of a rf-GD-MS.

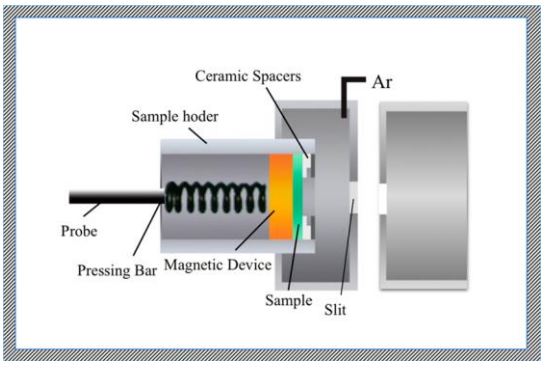

The rf-GD-MS experiments were carried out by applying rf power from 10 W up to 50 W. The discharge pressure was in the range of 1.3−8.0 mPa. The cell was precooled with liquidnitrogen to reduce the contaminations from C, N, and O elements. The low-intensity ion beams (below 10^{-13} A) were measured by an ion counter with a channeltron while the highintensity ion beams (above 10−13 A) were measured

by a Faraday cup. For most of the measurements, the working resolution was fixed at 3800.

2.4 Magnetic Field Simulation by Ansys Method

In order to compare the effects of the stacked magnets vs two block magnets, the magnetic field strength and its distribution was simulated using the software "Mechanical APDL (ANSYS) 14.0". A transverse block magnet (20 mm × 18 mm × 5 mm) and a stack of six stacked transverse magnets (20 mm × 3 mm × 5 mm for each) were chosen as the analysis objects. The coercivety of 876 kA/m and magnetic permeability of 1.05, typical for NdFeB magnets, were selected for this calculation.

Table 1. Certified concentration of constituents in NIST SRM 1831 and NIST SRM 620.

Constituent	Certified concentration in NIST SRM 1831	Certified concentration in NIST SRM 620
Na_2O	13.32	14.39
MgO	3.51	3.69
Al_2O_3	1.21	1.80
SO_3	0.25	0.28
CaO	8.20	7.11

RESULTS AND DISCUSSIONS

3.1 Optimization of Parameters for Signal Enhancement of the Stacked Magnets

Several literatures have reported that the influence of magnetic field on the GD discharge plasma strongly related to the discharge conditions.[17,18,22] Here, we demonstrate the effects of the magnetic field strength under different experiment conditions, namely, the discharge pressure and the rf-power.

The discharge pressure dependent magnetic enhancement results were shown in Figure 3. This study was performed with four different pairs of magnet pieces (n = 0, 2, 4, 6, and n = 0 meant no magnet piece applied). During the rf-GD-MS experiments, the pressure was varied from 1.3 to 8.0 mPa, while the rf power was fixed at 30 W. As shown in Figure 3, the signal intensities were gradually enhanced as the increasing of the pressure. This can be explained that by increasing the discharge pressure, the probability of creating argon ions and of their scattering with solid sample was increased. Moreover, with added stacked magnets, such an increase became more pronounced. This observation suggested that there was synergetic enhancement effects in the MS signal intensity. By
increasing the discharge pressure, the plasma density would increase, while the increase of the magnetic field strength could increase the sputter efficiency, since more ions could be produced.[8,22] When the discharge pressure was above 6.7 mPa, poor vacuum, some interferences, or redeposition might be caused.[24]

The rf-power dependence of the magnetic enhancement was studied using Y2O3, BSO, and BTN samples with rf-power in the range from 10 to 50 W under the discharge pressure of 5.3 mPa. Figure 4 indicated that the signal intensities were increased when the rf power was in the range of 10−50 W. The increase of rf power could increase both the ion densities and their kinetic energy since the negative self-biased potential is increased.[8,26] This would further result in improved sputtering and ionization efficiency. With the addition of magnetic field, the ion trajectory was bent and the plasma density would be further increased. However, in the case of rf power around 50 W, the crystal sample was observed to crack, which might be attributed to the poor heat conduction for nonconducting samples. Therefore, the discharge pressure and rf-power were optimized and fixed at 5.3 mPa and 30 W for the following studies.

3.2 Influences of the Stacked Magnets and the Block Magnet Methods on Signal Intensities

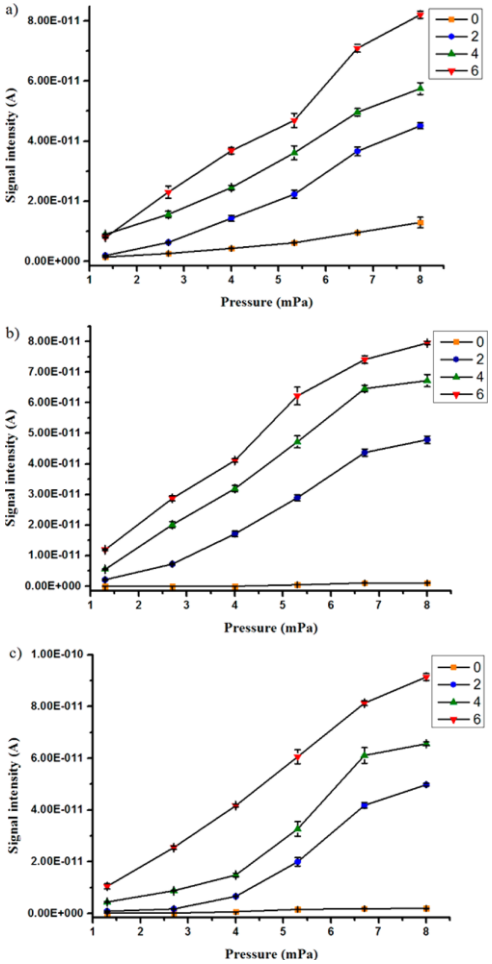

Figure 3. rf-GD-MS intensity of (a) matrix element Y in Y_2O_3, (b) matrix element Bi in BSO, and (c) matrix element Ba in BTN as a function of discharge pressure with constant

rf-power of 30 W and different pairs of magnet pieces (n = 0, 2, 4, 6) (signal intensity versus discharge pressure).

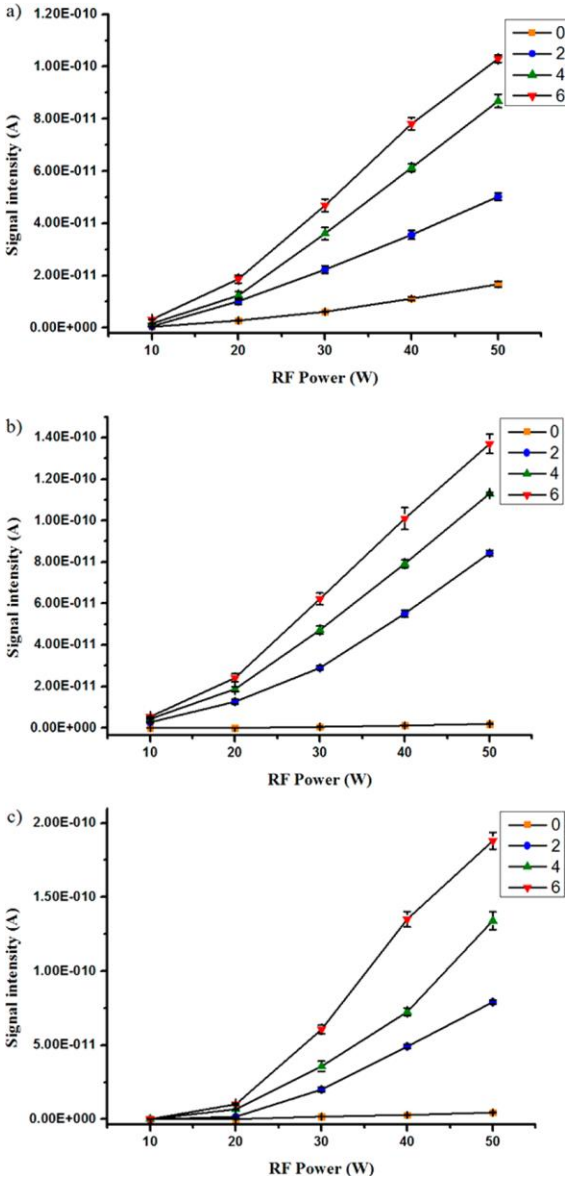

Figure 4. rf-GD-MS intensity of (a) Y in Y_2O_3, (b) Bi in BSO, and (c) Ba in BTN as a function of rf-power at the pressure of 5.3 mPa and different pairs of magnet pieces (n = 0, 2, 4, 6) (signal intensity versus rf-power).

To investigate and compare the influences of the stacked magnets and two block magnets (axial and transverse, as described in the Experimental Section), three insulators Y_2O_3, BSO, and BTN were used to test the rf-GD-MS signals. The MS measurements were carried out at 5.3 mPa discharge pressure and 30 W rf power. The signals of Y in the Y_2O_3 sample, Bi in the BSO sample, and Ba in the BTN sample were recorded using either block or stacked magnets.

Figure 5 showed that for Y, Bi, and Ba, the MS intensity obtained by the axial block magnet was about 1.1−4.6 times of that obtained in the absence of magnet applied, and the MS intensity obtained by the transverse magnet was about 14−135 times of that obtained in the absence of magnet applied. The result could suggest that the signal enhancement by axial magnet was not as notable as that using the transverse magnet. Meanwhile, six transverse stacked magnets (20 mm × 3 mm × 5 mm for each piece) and a transverse block magnet (20 mm × 18 mm × 5 mm) were used for further comparison. Although, the block and the stacked magnets offer the same magnetic field strength of 0.153 T, to our surprise, the results demonstrated that for Y, Bi, and Ba, the MS intensity was enhanced almost by a factor of 1.5−1.6 from the stacked magnetic pieces comparedto the transverse block magnet.

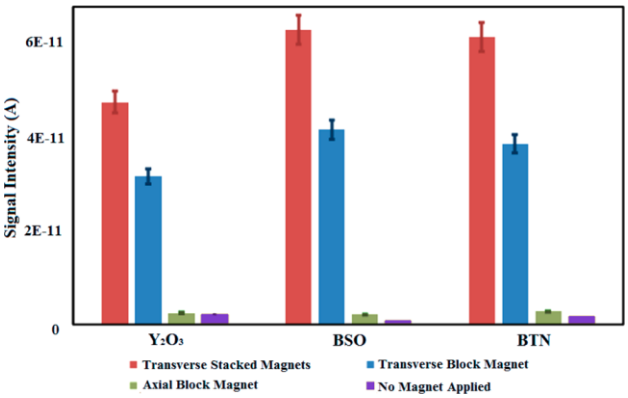

Figure 5. rf-GD-MS intensity of Y in Y2O3, Bi in BSO, and Ba in BTN with six stacked magnets, two block magnets, and without magnet applied.

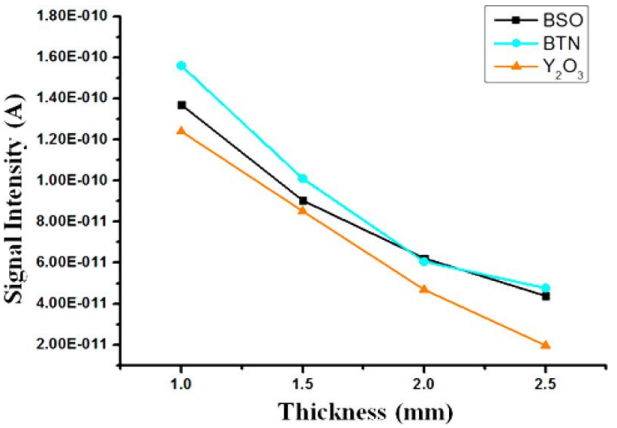

Figure 6. rf-GD-MS intensity of Y in Y_2O_3, Bi in BSO, and Ba in BTN as a function of sample thickness at a constant discharge pressure of 5.3 mPa and rf-power of 30 W.

The magnetic field enhancement in the sputtering and ionization process was directly related to the strength of the field.[27] In order to demonstrate the effects of the field strength, the signal intensity was measured as a function of sample thickness and number of the stacked magnets in constant discharge pressure and rf-power (5.3 mPa, 30 W). The measured signal intensity was shown in Figures 6 and 7. It was clear that the signal intensity was reducing as the thickness of the sample increased and increasing as the number of

the stacked magnets increased. Signal intensity was measured approximately to be inverse proportional to the r^2 and linear with n, where r was the distance from the magnet and n was the number of the stacked magnets. Similar observations were reported by M. J. Heintz et al. for a rf-GD-AES measurement[22] using a ring shaped magnet and D. Alberts et al. for an rf-GDOES measurement[18] using a cylindrical magnet. Therefore, the signal decrease with sample thickness could be ascribed to the decrease of the surface effective magnetic field strength and the decrease of the capacitance of the sample as the sample thickness increased. Since the influence of the axial block magnet was extremely faint, only the transverse block magnet and transverse stacked magnets were used for the next experiments and mechanism studies.

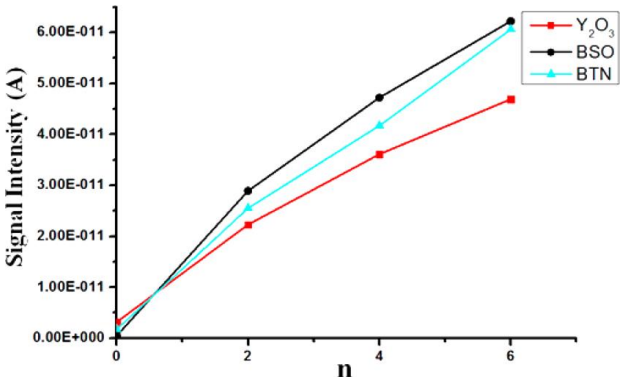

Figure 7. rf-GD-MS intensity of Y in Y2O3, Bi in BSO, and Ba in BTN as a function of the number of the magnet pieces at a constant discharge pressure of 5.3 mPa and rf-power of 30 W.

3.3 Accuracy and Stability of the Stacked Magnets Enhanced Method

Although it was clear that by adding stacked magnets could improve the signal intensity significantly, the accuracy of the method must be validated. The reference material, NIST1831, was used for measuring relative sensitivity factor (RSF) and detection limit of the magnetically enhanced (six stacked magnets) rf-GD-MS under 30 W rf power and 5.3 mPa gas flow pressure. The RSF was calculated with the certified concentrations (mass fractions) divided by the corresponding measured concentrations. The measured RSF values for selected elements, including Al, Ca, Mg, Na, and S are listed in Table 2.

The detection limits for six stacked magnets and a block magnet were compared first. The detection limits presented in Table 2 were calculated using the IUPAC definition:[28]

$$\text{detection limit} = 3\sigma_B/m$$

In this equation, σ_B represents the blank noise and m symbolizes the calibration curve slope. It was clear that the lowest detection limit obtained from the stacked magnets can reach 0.0082 μg g^{-1} while that from the block magnet was 0.020 μg g^{-1}, which was qualified to the analysis for trace elements and could improve the current limits of detection by the stacked magnets enhanced method.

Subsequently, the NIST 620 sample was used to measure the element concentration calibrated with RSF obtained from NIST 1831 in Table 2. The relative detection error was calculated by comparing the certified concentrations and the RSF calibrated concentrations. The results were shown in Table 3. The measured relative errors from the selected elements were in the range of 0.20−12%, which could validate the accuracy of the stacked magnets enhanced method.

Table 2. The measured concentration, RSF and detection limit of the elements in the sample NIST 1831. (relative to Si)

Elements	[a]Certified concentration C0(%)	Measured concentration C (%)	RSF(C0/C)	Detection Limit (ppm)
Al	1.88	10.58	0.18	0.93
Ca	17.16	12.42	1.38	1.1
Mg	6.21	3.18	1.95	0.0091
Na	28.92	28.89	1.00	1.6
S	0.30	0.49	0.61	0.0082

[a]Certified concentration of each element was directly calculated from the certified concentration of related oxides (Al_2O_3, CaO, MgO, Na_2O and SO_3) in the standard reference material NIST 1831

Table 3. Comparison of rf-GD-MS results of NIST 620 calibrated by RSF and the certified concentration. (relative to Si)

Elements	[a]Certified concentration (%)	Measured concentration C (%)	Calibrated concentration by RSF (%)	Relative error (%)
Al	2.83	14.31	2.57	-9.2
Ca	15.08	10.95	15.11	0.20
Mg	6.60	3.62	7.06	7.0
Na	31.69	34.03	34.03	7.4
S	0.33	0.61	0.37	12

[a]Certified concentration of each element was directly calculated from the certified concentration of related oxides(Al_2O_3, CaO, MgO, Na_2O and SO_3) in the standard reference material NIST 620

3.4 Stability of the Stacked Magnets Enhanced Method Using Typical Insulating Materials

To validate the stability of rf-GD-MS with stacked magnets, signal intensity of typical elements in Y_2O_3, BSO, and BTN samples were recorded against sputtering time. Experiments were carried out at 5.3 mPa gas flow pressure and 30 W rf-power with six stacked NdFeB magnets. The concentrations of Al, Zr, Eu, and Zn in Y_2O_3 were determined as 4.7×10^3 μg g^{-1}, 99 μg g^{-1}, 6.0 μg g^{-1},and 0.83 μg g^{-1}. The concentrations of Si, Al, Fe, and Cu in BSO were determined as 7.3×10^4 μg g^{-1}, 1.7×10^2 μg g^{-1}, 9.4 μg g^{-1}, and 4.1 μg g^{-1}, respectively. The concentrations of Nb, Ti, La, and Bi in BTN were determined as 3.7×10^5 μg g^{-1}, 5.2×10^4 μg g^{-1}, 9.1×10^4 μg g^{-1}, and 2.3 μg g^{-1}. The results indicated that the relative standard deviation (RSD) of typical elements of Y_2O_3, BSO, and BTN were within 13%, 15%, and 13%, respectively. Figure 8 further suggested that the discharge, sputtering, and ionization of each sample could be remained stable throughout the whole analysis process.

3.5 Studies on the Signal Intensity Enhancement Mechanism of rf-GD-MS by Using Stacked Magnets Method

So far, our experimental results demonstrated that adding stacked magnets could increase the signal intensity by almost a factor of 1.5−1.6 in comparison with a block magnet. In order to establish the possible enhancement mechanism and explain the difference between stacked magnets and block magnet, the distribution of magnetic flux density were simulated and calculated using the software "Mechanical APDL (ANSYS) 14.0". The simulation results were shown in Figure 9, and they indicated that the stacked magnets had a distinct oscillating distribution of magnetic field which was different from the block magnet. What is more important is that the peaks of the oscillating magnetic field were in the range of 1.04 T to 1.17 T, while no obvious oscillating field distribution was found for the block magnet. The oscillating behavior was further determined by the boundaries between the stacked magnets. As shown in Figure 9b, the segments of the individual magnet could be clearly identified. On the other hand, for a block magnet, the field was concentrated on the edge of the magnet without clear oscillating field distribution.

The oscillating magnetic distribution with high peak intensity would be responsible for the high signal intensity in rf-GD-MS. At the relatively low magnetic fields employed in glow discharge spectroscopy, only electron trajectories were significantly affected as ions are much heavier and their paths more difficult to alter.29−31The comparisons of the electron trajectories based on different configuration of the magnets were illustrated in Figure 10. There were two possible effects in boosting the signal intensity. First, the increased oscillating magnetic field could obviously extend the movement trajectories of the charged particles, especially for the electrons, as shown in Figure 10b,c. Second, the increased movement of electrons would improve the collisions between the ions and neutral particles, which could help achieve more efficient sputtering and ionization efficiency.

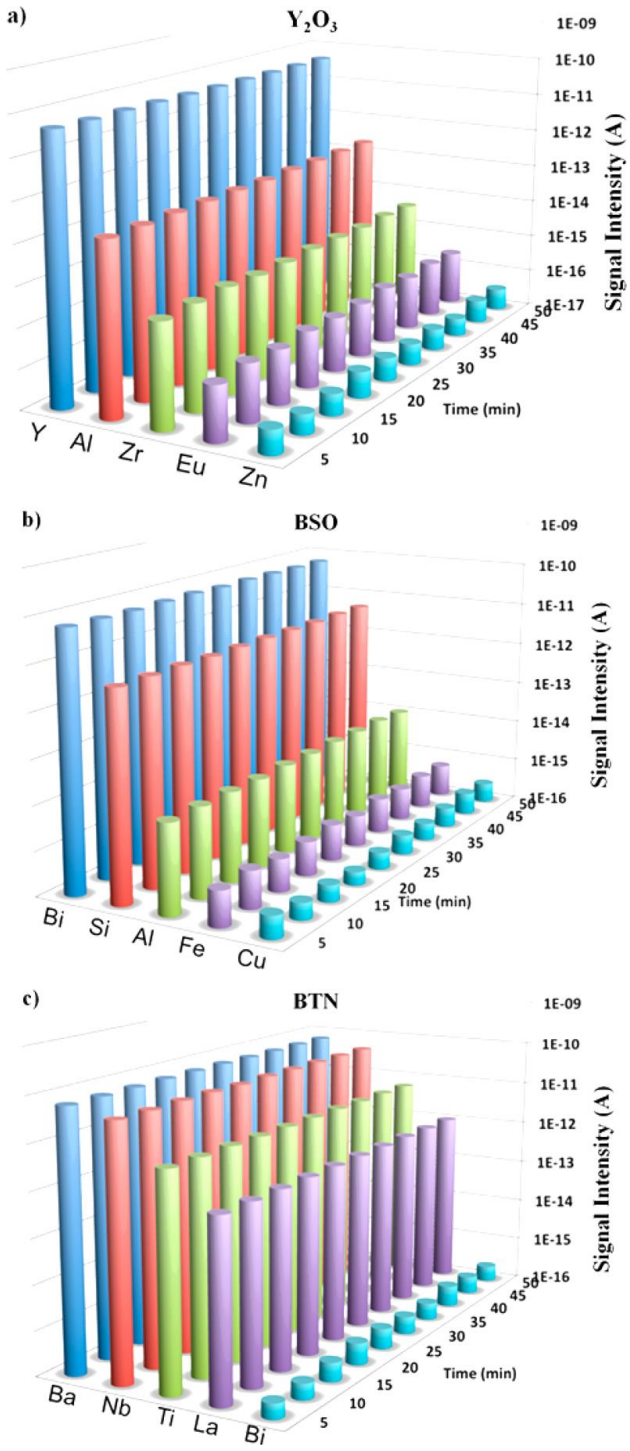

Figure 8. Stability of the discharge, represented by the signal intensity of the typical elements, as measured during sputtering of (a) Y_2O_3, (b) BSO, and (c) BTN using the stacked magnets.

Thus, the oscillating magnetic field could extend the movement path of electrons and increase the collision between the electrons and neutral particles to increase the ionization efficiency. However, such effects were much weaker

for a block magnet, as shown in Figure 10a. Therefore, as the sputtering and ionization of the sample were significantly enhanced by the stacked magnets method, the detected MS signals from the sample would also be increased accordingly.

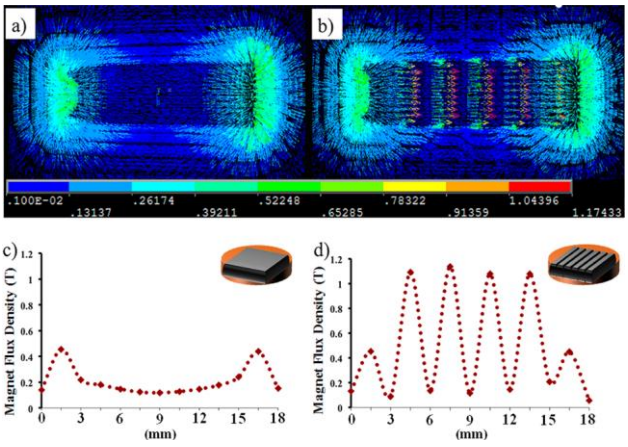

Figure 9. Ansys simulated the magnetic field distribution in cross section of (a) the transverse block magnet, (b) the six transverse stacked magnets and magnetic flux density of the (c) the transverse block magnet and (d) the six transverse stacked magnets (X-axis represented the points selected from the left to right side of the magnets along the 18mm direction)

CONCLUSION

In our present work, significant signal intensity enhancement was observed using the stacked magnets in rf-GD-MS for nonconducting samples. The enhancement of signal intensity was investigated as a function of discharge pressure, rf power, sample thickness, and number of the stacked magnets. The six stacked magnets could increase the signal intensity almost by a factor of 1.5−1.6 compared to the transverse block magnet.

The accuracy and detection limit of the stacked magnets method were validated using NIST samples 1831 and 620. The relative errors were calculated within 13% and the lowest detection limit could reach 0.0082 μg g−1, which indicated that the detection limit was significantly improved by the stacked magnets method. Moreover, the stability of this method was studied using ceramic and crystal samples. The relative standard deviation of the typical elements was within 15%, which indicated that the discharge, sputtering, and ionization could remain stable throughout the whole analysis process by using the stacked magnets method.

The possible mechanism for signal enhancement was further elucidated by Ansys magnetic field simulation. The results suggested that the stacked magnets offered a distinct oscillating magnetic distribution with high peak intensity. This would extend the movement path of electrons and enhance the collisions between the electrons and neutral particles to further increase the efficiency of ionization. Thus, the overall signal intensity would be increased accordingly. Further studies in this area are being carried out in our laboratory.

AUTHOR INFORMATION

Corresponding Authors

*Phone: +86215241301, Fax: +862152415609, E-mail: qianrong@mail.sic.ac.cn,
*Phone: +441273678492, Fax: +441273876687, E-mail: qiao.chen@sussex.ac.uk

Author Contributions

The manuscript was written through contributions of all authors. All authors have given approval to the final version of the manuscript.

Notes

The authors declare no competing financial interest.

ACKNOWLEDGMENT

The authors greatly acknowledge the financial support by the National Natural Science Foundation of China (no. 51472261), Youth Innovation Promotion Association CAS and the National Basic Research Program of China (no. 2012CB720900).

REFERENCES

(1) Molle, C.; Wautelet, M.; Dauchot, J. P.; Hecq, M. J. Anal. At. Spectrom. 1995, 10, 1039−1045.

(2) Pisonero, J.; Costa, J. M.; Pereiro, R.; Bordel, N.; Sanz-Medel, A. Anal. Bioanal. Chem. 2004, 379, 17−29.

(3) Pisonero, J.; Feldmann, I.; Bordel, N.; Sanz-Medel, A.; Jakubowski, N. Anal. Bioanal. Chem. 2005, 382, 1965−1974.

(4) Bouza, M.; Pereiro, R.; Bordel, N.; Sanz-Medel, A.; Fernández, B. J. Anal. At. Spectrom. 2015, 30, 1108−1116.

(5) Pisonero, J.; Valledor, R.; Licciardello, A.; Quirós, C.; Martín, J. I.; Sanz-Medel, A.; Bordel, N. Anal. Bioanal. Chem. 2012, 403, 2437−2448.

(6) Pisonero, J. Anal. Bioanal. Chem. 2006, 384, 47−49.

(7) Marcus, R. K. J. Anal. At. Spectrom. 2000, 15, 1271−1277.

(8) Gibeau, T. E.; Marcus, R. K. J. Anal. At. Spectrom. 1998, 13, 1303−1311.

(9) Saprykin, A. I.; Becker, J. S.; Crone, U. v. d.; Dietze, H.-J. Fresenius' J. Anal. Chem. 1997, 358, 145−147.

(10) Becker, J. S.; Westheide, J.; Saprykin, A. I.; Holzbrecher, H.; Breuer, U.; Dietze, H.-J. Microchim. Acta 1997, 125, 153−160.

(11) Jäger, R.; Becker, J. S.; Dietze, H.-J.; Broekaert, J. A. C. Fresenius, J. Anal. Chem. 1997, 358, 214−217.

(12) Shick, C. R., Jr.; DePalma, P. A., Jr.; Marcus, R. K. Anal. Chem. 1996, 68, 2113−2121.

(13) Muñiz, A. C.; Pisonero, J.; Lobo, L.; Gonzalez, C.; Bordel, N.; Pereiro, R.; Tempez, A.; Chapon, P.; Tuccitto, N.; Licciardello, A.; Sanz-Medel, A. J. Anal. At. Spectrom. 2008, 23, 1239−1246.

(14) Duckworth, D. C.; Donohue, D. L.; Smith, D. H.; Lewis, T. A.; Marcus, R. K. Anal. Chem. 1993, 65, 2478−2484.

(15) Winchester, M. R.; Payling, R. Spectrochim. Acta, Part B 2004, 59, 607−666.

(16) Vega, P.; Pisonero, J.; Bordel, N.; Tempez, A.; Ganciu, M.; Sanz-Medel, A. Anal. Bioanal. Chem. 2009, 394, 373−382.

(17) Vega, P.; Valledor, R.; Pisonero, J.; Bordel, N. J. Anal. At. Spectrom. 2012, 27, 1658−1666.

(18) Alberts, D.; Therese, L.; Guillot, P.; Pereiro, R.; Sanz-Medel, A.; Belenguer, P.; Ganciu, M. J. Anal. At. Spectrom. 2010, 25, 1247−1252.

(19) Jakubowski, N.; Dorka, R.; Steers, E.; Tempez, A. J. Anal. At. Spectrom. 2007, 22, 722−735.

(20) Pisonero, J.; Fernández, B.; Günther, D. J. Anal. At. Spectrom. 2009, 24, 1145−1160.

(21) Saprykin, A. I.; Becker, J. S.; Dietze, H.-J. Fresenius' J. Anal. Chem. 1997, 359, 449−453.

(22) Heintz, M. J.; Hieftje, G. M. Spectrochim. Acta, Part B 1995, 50, 1109−1124.

(23) Cho, W. B.; Kim, M. Y.; Kim, H. J. Microchem. J. 2000, 64, 41−50.

(24) Bentz, B. L.; Harrison, W. W. Anal. Chem. 1982, 54, 1644−1646.

(25) Ming, C.; Jianshi, R.; Hongbo, M.; Zhang, G. Spectrochim. Acta, Part B 1997, 52, 1161−1166.

(26) Luesaiwong, W.; Marcus, R. K. J. Anal. At. Spectrom. 2004, 19, 345−353.

(27) Heintz, M. J.; Broekaert, J. A. C.; Hieftje, G. M. Spectrochim. Acta, Part B 1997, 52, 579−591.

(28) Long, G. L.; Voigtman, E. G.; Kosinski, M. A.; Winefordner, J. D. Anal. Chem. 1983, 55, 1432−1434.

(29) Hassouba, M. A. Eur. Phys. J.: Appl. Phys. 2001, 14, 131−135.

(30) Pekker, L.; Krasheninnikov, S. I. Phys. Plasmas 2000, 7, 382−390.

(31) Li, J.; Chen, Q. M.; Li, Z. G. J. Phys. D: Appl. Phys. 1995, 28,1121−1125.